ADVANCED MATERIALS

Supporting Information

for *Adv. Mater.,* DOI: 10.1002/adma.202104406

Electrical Generation and Deletion of Magnetic Skyrmion-Bubbles via Vertical Current Injection

*Seungmo Yang, Kyoung-Woong Moon, Tae-Seong Ju, Changsoo Kim, Hyun-Joong Kim, Juran Kim, Bao Xuan Tran, Jung-Il Hong, and Chanyong Hwang**

WILEY-VCH

Supporting Information

Electrical Generation and Deletion of Magnetic Skyrmion-bubbles Via Vertical Current Injection and Its Application to Skyrmion Racetrack Memory

Seungmo Yang[†], *Kyoung-Woong Moon*[†], *Tae-Seong Ju*[†], *Changsoo Kim, Hyun-Joong Kim, Juran Kim, Bao Xuan Tran, Jung-Il Hong, and Chanyong Hwang**

Supporting Information 1: Choice for Oxide Layer on the Magnetic Channel

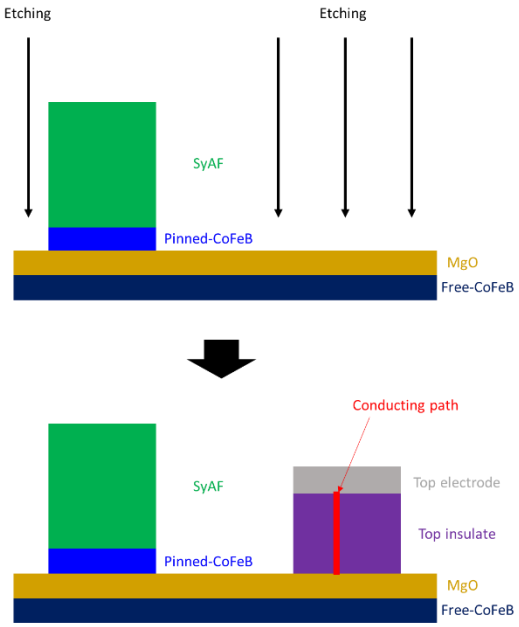

Supporting Figure 1. Possible skyrmion racetrack memory structure.

The complicated triple oxide layer was used for the experiment because we were not able to fabricate the three-terminal structure in one-step fabrication process. That is, we fabricated the magnetic channel of W/CoFeB/Ta/MgO/Ta (capping) first, where the Ta capping is fully oxidized after breaking the vacuum. Then, the only reason we chose GdO_x as the top insulating layer is because it is a well-known oxide layer where the oxygen vacancies are highly mobile. We believe that the conducting path is very similar to the filament introduced in resistive RAM (ReRAM) technology. Therefore, we think that many other oxide layers used in the ReRAM research field can be used in our structure with a single-layer oxide layer geometry.

However, from an application point of view, for achieving a high TMR (tunnel magnetoresistance), the oxide layer adjacent to the CoFeB layer must be MgO. Therefore, **Figure S1** can be used for realization of skyrmion racetrack memory in the future.

Supporting Information 2: The Vertical Conducting Path and Consequent Current Distribution

In the main paper, we utilized a vertical conducting path to generate and annihilate isolated skyrmion-bubbles as shown in Figure 1d. To verify the presence of the vertical conducting path and the consequent current distribution in the magnetic film, we observed the stripe pattern change upon current injection. The initial state is a completely random stripe domain pattern. MOKE images of a stripe domain pattern after applying a positive and negative V_v pulse, respectively, are presented in **Figure S2**a and S2b. A positive V_v pulse creates a concentric stripe domain pattern centered on the conducting path (red square), whereas a negative V_v pulse forms a stripe domain pattern in the form of being absorbed into the conducting path, as described in Figure S2a and S2b. The stripe domains in Figure S2a and S2b can be explained by considering a radial current flow.[1] The radial current flow is generated when the vertical current reaches the magnetic film through the narrow conducting path. The radial current density decays with the distance *r* from the conducting path, leading to the SOT decay with *r*. For a domain wall tilted clockwise (Figure S2c), the spreading current flow from the center exerts an outward SOT force on the tilted domain wall. As the SOT force is inversely proportional to *r*, the force on the right edge is larger than that on the left edge, as described in Figure S2c. That is, the spreading radial current makes the domain wall parallel to the tangent of a concentric circle. By contrast, the current "absorbed" into the center exerts an inward SOT force on the domain wall. In this case, the larger SOT force exerted on the right edge makes the domain wall perpendicular to the tangent of a concentric circle. The oppositely tilted domain walls lead to the same result as shown in Figure S2e and S2f. Therefore, the radial current by a positive V_v pulse forms the concentric circle shape of a stripe domain, whereas the current absorbed creates a stripe pattern that gathers into the center, as shown in Figure S2g and S2h. The videos for stripe domain evolution by a positive

and negative V_v pulse are provided in Supporting movie 1 and 2, respectively. Thus, the presence of the vertical current path and the corresponding current distribution in the film can be confirmed by the stripe domain patterns formed by the positive and negative pulses.

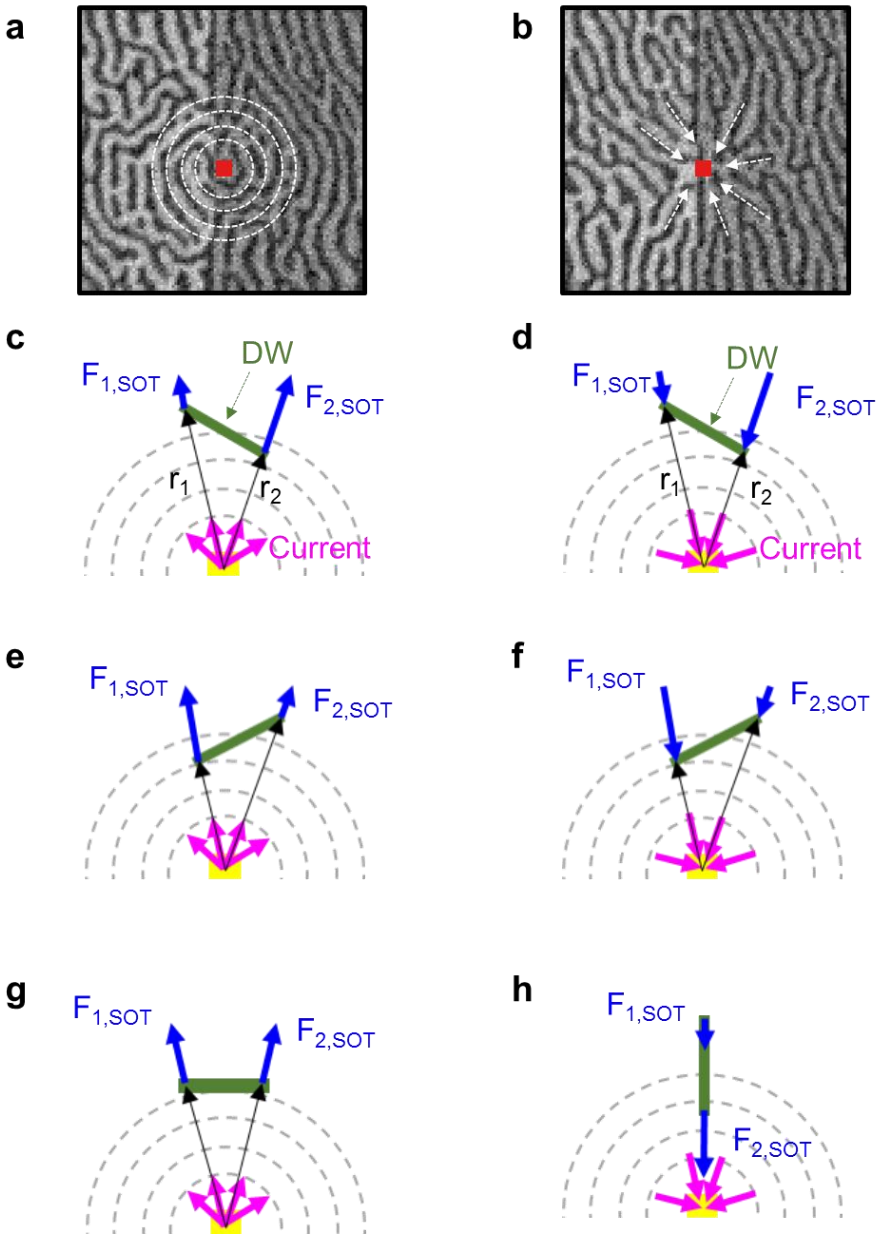

Supporting Figure 2. a, b) MOKE images of a stripe domain pattern after applying a) a $+V_v$ pulse and b) a $-V_v$ pulse. c–h) SOT forces exerted on various types of domain walls.

Supporting Information 3: Skyrmion-Bubble Stability under a Certain *z*-Axis Magnetic Field

We have chosen the magnitude of the *z*-axis magnetic field ($\mu_0 H_z$) as 0.43 mT for all experiments in this article based on skyrmion-bubble stability. A previous report[2] introduced a method of generating a bunch of skyrmion-bubbles by applying a tilted magnetic field and returning to the certain $\mu_0 H_z$ (0.43 mT), as described in **Figure S3**a. An image of the created skyrmion-bubbles under the 0.43 mT $\mu_0 H_z$ is presented in Figure S3b, indicating that isolated skyrmion-bubbles are stable under the 0.43 mT $\mu_0 H_z$.

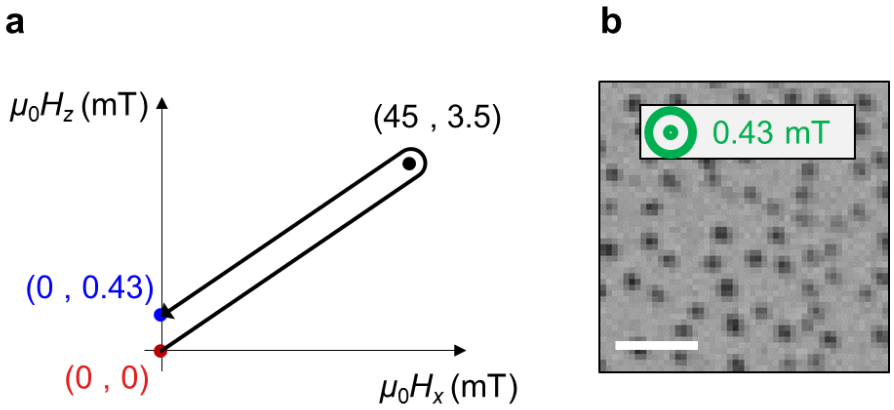

Supporting Figure 3. a) A route of applying a magnetic field for generating a bunch of skyrmion-bubbles based on a previous report.[2] b) MOKE image of the generated skyrmion-bubbles after applying a magnetic field. Scale bar, 5 μm.

Supporting Information 4: Asymmetric Behavior of Skyrmion-bubble Generation

If there is an asymmetry in current distribution due to the position of source/drain, more skyrmion bubbles can be created in a certain direction. This phenomenon can be simply reproduced by simulation. As in the experiment, when the current exit location is limited, the current injected into the conduction path spreads radially in the vicinity of the injection spot and then changes to a uniform *x*-direction current at a distance. It is simply assumed that in this situation, a uniform current in the *x*-direction is added to the radial current. **Figure S**4 shows the results.

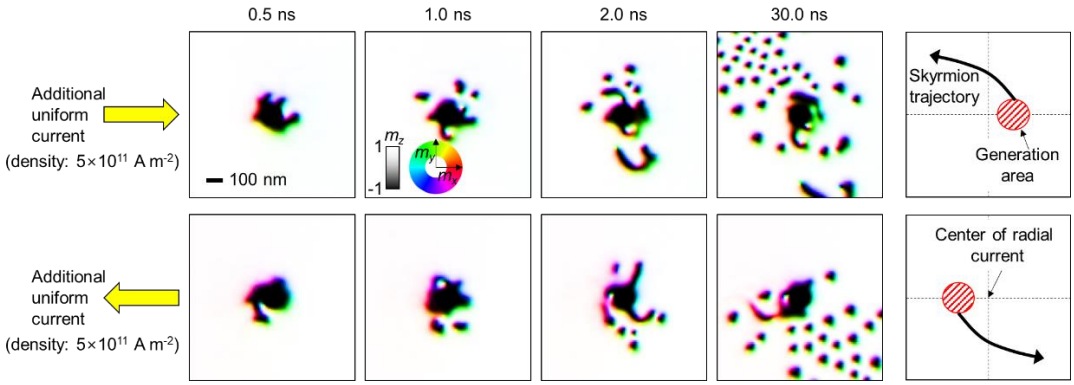

Supporting Figure 4. Micromagnetic simulation result under both spreading and additional currents.

In places where the radial and uniform currents are added to each other (red shaded area), skyrmion bubbles are formed more easily, and where they cancel each other, their generation is suppressed. The formed skyrmion bubbles are moved by the current, and at the same time, the skyrmion Hall effect occurs. Therefore, skyrmion bubbles accumulate on one side of the sample. The aforementioned result has a larger skyrmion Hall effect than does the experimental result because the current density is high. Therefore, if the current has directionality, it also affects the direction in which the skyrmion bubbles are accumulated, and this is similar to the experimentally confirmed result. However, the breaking of the stripe

domain, the core principle of the formation of the skyrmion bubble, should occur in the same way.

Supporting Information 5: An Example File for MuMax3 for Micromagnetic Simulations

This is an example file of MuMax3 for Figure 2d–i.

```
Nx := 400

Ny := 400

c := 2e–9

holej := 3.0e–3

fixedr := 50e–9

thick := 5e–9

setgridsize(Nx, Ny, 1)

setcellsize(c, c, 1e-9)

grainSize    := 5e-9

randomSeed := 1

maxRegion    := 199

ext_makegrains(grainSize, maxRegion, randomSeed)

defregion(200, cylinder(fixedr, fixedr).transl(0,0,0))

Msat = 1000e3

Aex = 1.0e-11

Dind = -2.0e-3

anisU = vector(0, 0, 1)

B_ext = vector(0, 0, 0.15)

lambda = 1

Pol = 0.1

epsilonprime = 0

frozenspins.setregion(200,1)
```

```
m = uniform(0,0,1)
m.setregion(200, uniform(0,0,-1))
for i:=0; i<maxRegion; i++{
	K := 680000
	Ku1.SetRegion(i, K + randNorm() * 0.10 * K)
}
for i:=0; i<maxRegion; i++{
	for j:=i+1; j<maxRegion; j++{
		ext_ScaleExchange(i, j, 0.9)
	}
}
mask1 := newVectorMask(Nx, Ny, 1)
mask2 := newVectorMask(Nx, Ny, 1)
for i := 0; i < Nx; i++ {
	for j := 0; j < Ny; j++ {
		r := index2coord(i, j, 0)
		x := r.X()
		y := r.Y()
		dist := sqrt(x*x + y*y)
		jrad := holej/thick*1/(2*pi*dist)
		sx := -y / dist
		sy := x / dist
		mask2.setVector(i, j, 0, vector(sx, sy, 0))
		mask1.setVector(i, j, 0, vector(0, 0, jrad))
	}
```

```
}

alpha = 0.5

run(0.5e–9)

alpha = 0.1

FixedLayer.Add(mask2, 1)

J.Add(mask1, 1)

t = 0

run(50e–9)
```

Supporting Information 6: Additional Supporting Phenomena for Skyrmion-Bubble Generation Via Vertical Current Injection

The first supporting scenario considers temperature-dependent phase transitions. In the conducting path region where the current is concentrated, the magnetic material can be in a paramagnetic state due to high temperatures. The paramagnetic state consists of misaligned magnetization vectors, and therefore, if a local region is seen, there are more topological charges than in the ferromagnetic state. That is, there would be numerous topological charges near the conducting path. The SOT pushes out the magnetization states near the conducting path. Therefore, the topological charges near the electrode are pushed outwards and become skyrmion-bubbles that can be observed. This is shown schematically in **Figure S**6a.

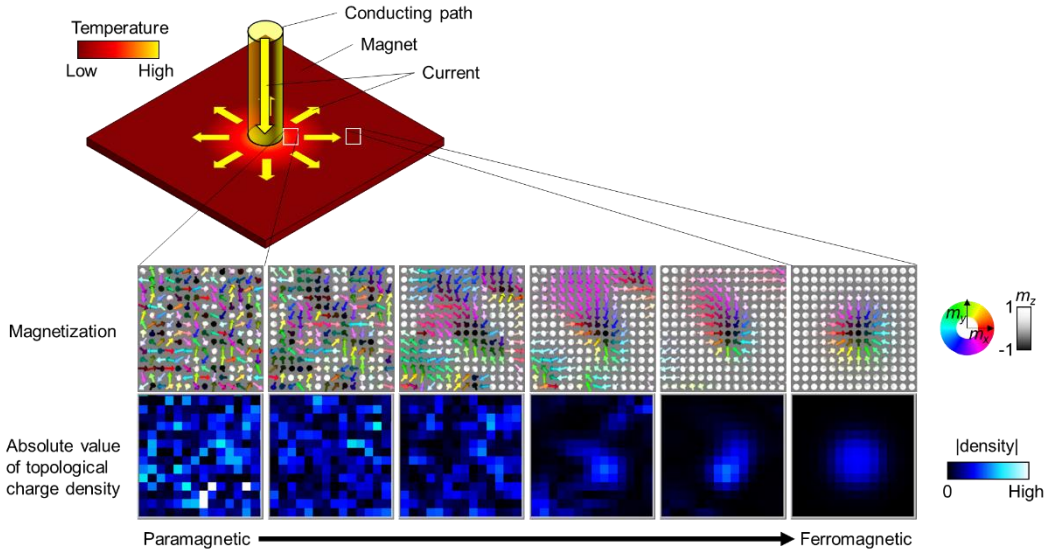

Supporting Figure 6a. Schematics of topological charge analysis.

The second mechanism is based on temperature distribution due to the current and strip–bubble–uniform phase changes because of the perpendicular magnetic field. Results of both Saratz et al.[3] and Meier et al.[4] show that increasing the perpendicular magnetic field of a sample changes its stripe domains observed at the zero field to a stripe–bubble–uniform state. Moreover, as the temperature increases, the range of perpendicular magnetic fields in which

stripe–bubble–uniform states are observed increases (see Figure S6b). Thus, even if a uniform perpendicular magnetic field (cyan line) is applied, the condition around the conducting path can be stabilized in the stripe domain phase, while the bubble state can be stabilized at a distance. The SOT pushes the stripe domains outwards, and when a stripe domain enters the bubble region, the stripe domain breaks, forming a bubble of skyrmion bubbles.

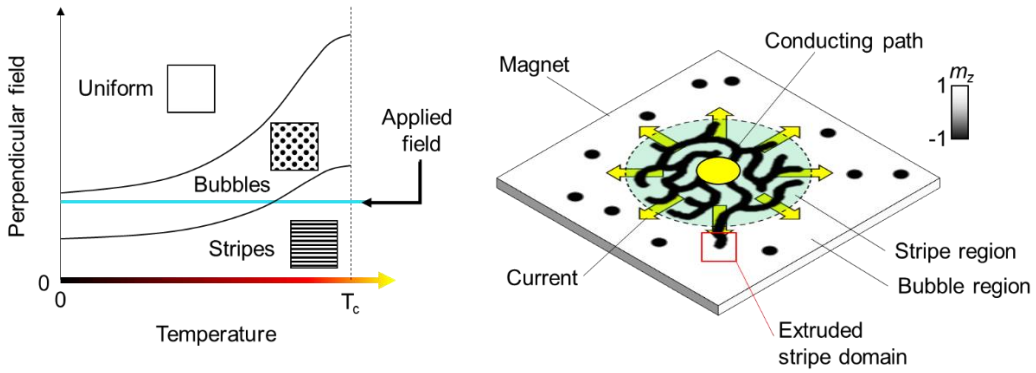

Supporting Figure 6b. Schematics of temperature-dependent ground states analysis.

The third scenario is based on the Oersted field. This may also include the field-like SOT. The perpendicular current creates a vortex-type Oersted field around it.[5] The strength of this Oersted field decreases as it moves away from the conducting path. According to a recent study,[2] the application of an in-plane magnetic field to the perpendicular magnetization samples widens the range of perpendicular magnetic fields in which stripe–bubble–uniform phases exist. Thus, even if a uniform perpendicular magnetic field is applied, stripe domains can exist only around the conducting path, and bubble domains can exist at a distance. The SOT pushes the stripe domains outwards, and when a stripe domain enters the bubble region, the stripe domain breaks, forming a bubble of skyrmion-bubbles, as mentioned in the second mechanism.

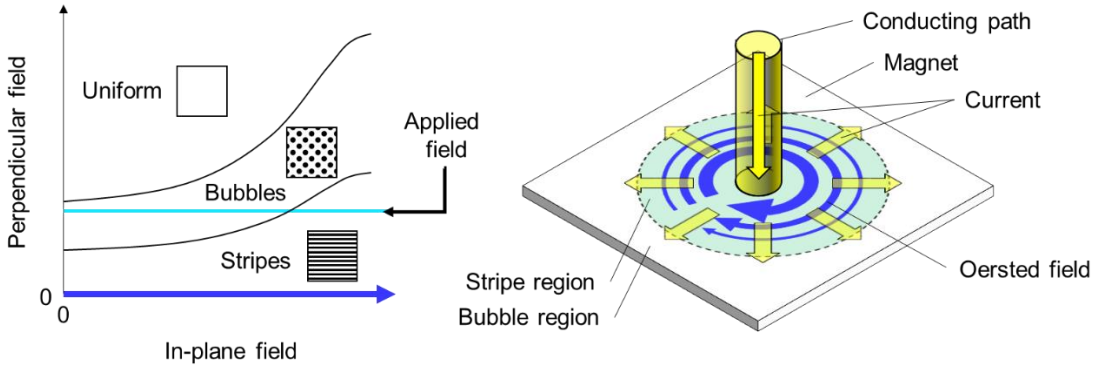

Supporting Figure 6c. Schematics of in-plane Oersted field analysis.

The fourth scenario is oxygen migration during the conducting path generation. Because the PMA in CoFeB/MgO originates from Fe–O bonding, oxygen vacancy migration can deteriorate the PMA in the region under the conducting path. Reduced PMA is the same effect as those by Joule heating and the Oersted field.

These four mechanisms are assumed to aid in the formation of skyrmion-bubbles. However, it is imperative that magnetization states are pushed outwards by the current. The proposed simulations in the article show that skyrmion-bubbles are formed when magnetization states are pushed outwards by the current.

Supporting Information 7: Stochastic Behavior in Generating Skyrmion Bubbles

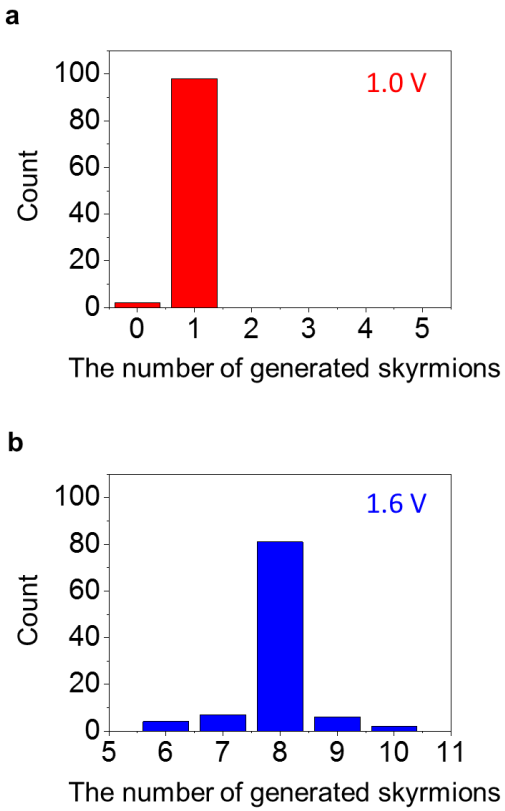

Supporting Figure 7. Histogram for 100 times generation of skyrmion-bubbles with a) 1.0 and b) 1.6 V pulses.

Supporting Information 8: Suggestion for a Possible Fabrication Process of a Vertical Conducting Path

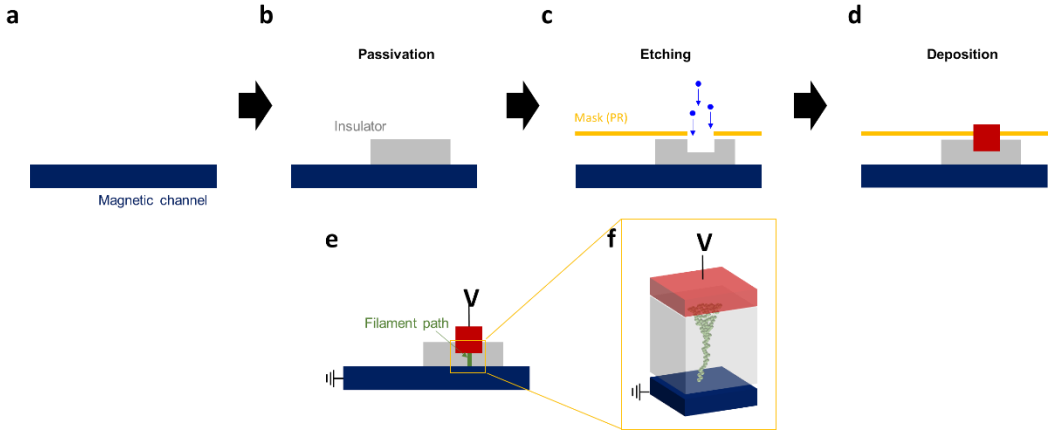

Supporting Figure 8. Fabrication process of a filament-based vertical conducting path.

The simplest method is to fabricate a vertical metal electrode directly. However, based on the proposed concept in this article, to generate a spreading or inhaling current, the vertical conducting path has to be much smaller than the track width. If the vertical conducting path is fabricated directly by a vertical metal electrode, the feature size is defined as the diameter of the vertical metal electrode. This causes the entire area of the racetrack memory device to be very large, because the track width requires a large number of the feature size.

To avoid this issue, we propose filament-based vertical conducting path generation, which has been well-established for resistive random access memory technology. The fabrication process for creating a vertical filament path in a confined region is described in **Figure S8**a–d. Here, the feature size is the width of the top electrode (red). In the structure in Figure S8e, applying voltage via the top electrode (red) induces a filament path at the region marked by the yellow box because the induced electric field is strongest in the region owing to the short distance between the top and bottom electrodes. Once a filament path is connected, no further paths are created because a voltage drop occurs via the already generated conducting path. In addition, the diameter of a generated filament path is much

smaller than the top electrode width (the feature size). Therefore, the entire area of the device can be small because the track width is determined based on the filament path diameter.

Supporting Information References

[1] J. Gorchon, J. Curiale, A. Cebers, A. Lemaître, N. Vernier, M. Plapp, V. Jeudy, *Phys. Rev. B* **2015**, *92*, 060411.

[2] K.-W. Moon, S. Yang, T.-S. Ju, C. Kim, B. S. Chun, S. Park, C. Hwang, *NPG Asia Mater.* **2021**, *13*, 20.

[3] N. Saratz, U. Ramsperger, A. Vindigni, D. Pescia, *Phys. Rev. B* **2010**, *82*, 184416.

[4] T. N. G. Meier, M. Kronseder, C. H. Back, *Phys. Rev. B* **2017**, *96*, 144408.

[5] M.-W. Yoo, D. Rontani, J. Létang, S. Petit-Watelot, T. Devolder, M. Sciamanna, K. Bouzehouane, V. Cros, J.-V. Kim, *Nat. Commun.* **2020**, *11*, 601.